energies

Article

Analysis of the Heat Transfer in Electronic Radiator Filled with Metal Foam

Xiaofang Shan [1], Bin Liu [1,*], Zongsheng Zhu [1], Rachid Bennacer [2,*], Rounan Wang [1] and Panagiotis E. Theodorakis [3]

1 Tianjin Key Lab of Refrigeration Technology, Tianjin University of Commerce, Tianjin 300134, China
2 LMPS, ENS Paris-Saclay, CentraleSupélec, Université Paris-Saclay, CNRS, 91190 Gif-sur-Yvette, France
3 Institute of Physics, Polish Academy of Sciences, Al. Lotników 32/46, 02-668 Warsaw, Poland
* Correspondence: lbtjcu@tjcu.edu.cn (B.L.); rachid.bennacer@ens-paris-saclay.fr (R.B.)

Abstract: The performance of an electronic radiator filled with metal foam with a porosity of 96% was studied. The effect of the factors including the flow rates, the pores per linear inch (PPI) and the numbers of fins was analyzed. The results show that the electronic radiator with metal foam reflects a stronger ability of the heat transfer compared to the electronic radiator without metal foam. With the increase in the flow rate between 10 L/h and 60 L/h, the heat transfer coefficient of both of the two electronic radiators will be improved, but it is also dependent on the number of fins. In this study, we find that the heat transfer coefficient first increases and then decreases with the number of fins. The optimum number is three. As for the effect of the PPI, the higher the PPI, the larger the heat transfer coefficient, while the pressure drop always increases with the flow rates' increase, the pores per linear inch (PPI) and the numbers of fins.

Keywords: metal foam; electronic radiator; enhancement of heat transfer; pressure drop

check for updates

Citation: Shan, X.; Liu, B.; Zhu, Z.; Bennacer, R.; Wang, R.; Theodorakis, P.E. Analysis of the Heat Transfer in Electronic Radiator Filled with Metal Foam. *Energies* **2023**, *16*, 4224. https://doi.org/10.3390/en16104224

Academic Editors: Marco Marengo, Artur Bartosik and Dariusz Asendrych

Received: 25 January 2023
Revised: 10 May 2023
Accepted: 17 May 2023
Published: 20 May 2023

1. Introduction

With the rapid development of electronic technology, miniaturization and intelligence have become important directions in the development of contemporary equipment. The size of the electronic devices used in industrial production equipment is gradually decreasing, and the chip achieves a continuous increase in the operating frequency as well as integration density. This leads to a rapid increase in the heat flow density of the chip, and its temperature directly affects the stability of the performance. As a result, higher demands are placed on the thermal design of electronic chips. To ensure the operational stability of electronic devices, higher requirements for the reliability of electronic equipment are required. Through a high standard of thermal design work arrangements, reasonable cooling methods are chosen to ensure that the heat escaping from the device is removed from the surface more quickly and that the temperature around the component is always within the safe operating temperature range.

In recent years, metal porous materials have been used due to their unique properties and the combination of structural and functional material properties [1–3]. Widely used in biological, medical [4–6], aerospace [7] and industrial applications [8–12], the high demand for green materials in various fields has driven the development of metal foam. Porous metal foam structures with high specific surface area, high permeability properties and high mechanical strength are being explored as an alternative material to conventional heat exchangers. In the field of heat transfer [13–16], metal foam holds great promise for applications in multifunctional heat exchangers [17–19], cooling systems [20–23], high-power batteries, compact electronic heat sinks [23–28] and so on. Porous metal foam can significantly reduce the size and mass of equipment when used in heat transfer equipment due to their light mass and low density. They have great potential for application in industrial production as well as in related fields such as high technology, gaining more attention and importance.

The use of metal foam as a new compact heat exchanger has been investigated by numerical simulations. Chen et al. [13] presented a three-dimensional numerical simulation to reveal the flow and heat transfer characteristics of a new tube bundle design covered with metal foam. The results showed that tube bundles covered with metal foam with low porosity and low pore density have a strong advantage over bare tube bundles. For example, Kotresha et al. [16] discussed a numerical simulation of a metal foam heat exchanger system performed by a commercial software. The aim is to improve the thermal performance of the heat exchanger by reducing the pressure drop and increasing the heat transfer rate to the maximum.

Metal foam has also been investigated experimentally. Kim et al. and Shen et al. [14,15] found that the use of metal foam significantly reduces the overall thermal resistance compared to a conventional finned heat pipe heat sink. Hsieh et al. [29] experimentally investigated the effects of porosity, pore density (PPI) and air flow rate on the heat transfer characteristics of the aluminum foam heat sinks and found that the increase in porosity and pore density enhanced the non-local thermal equilibrium phenomenon. Liu et al. [30], based on the Reynolds number range of the equivalent spherical diameter of the foam from 32 to 1289, found that the porosity range was 0.87 to all seven types of the aluminum foams, and an empirical Equation was developed to relate the unexpected pressure drop to the unexpected flow rate. Dukhan et al. [31] presented heat transfer measurements within a rectangular block of commercially available aluminum foam subjected to constant heat flow on one side. The temperature profile decays in an exponential fashion as the distance from the heat base increases. Boomsma and Poulikakos [32] experimentally showed that varying the fluid conductivity has a relatively small effect on increasing the effective heat transfer rate.

The heat transfer performance of metal foam under forced convection and natural convection conditions has also been investigated by researchers. Shih et al. [33,34] demonstrated that under impact jet flow conditions for all values of jet–jet spacing, an increase in the pore density was accompanied by an increase in the heat transfer. Bhattacharya et al. [35] investigated forced convection heat transfer in a new finned metal foam heat sink, showing that when fins were added to the metal foam, the heat transfer was significantly enhanced, and the heat transfer coefficient increased with the number of fins until the addition of more fins would lead to the interference with the thermal boundary layer and retard heat transfer. Shen et al. [15] conducted a systematic study and analysis of the thermal and flow characteristics at different air speeds and thermal powers through experiments. It was found that the introduced metal foam significantly reduced the overall thermal resistance by 25.5% compared to a conventional finned heat pipe heat sink.

This paper focuses on the implementation of enhanced heat transfer analysis for metal-filled radiator components with 96% porosity and 10 PPI pore density of copper foam, aluminum foam and 20 PPI pore density of copper foam. The heat transfer performance of the devices at different flow rates and at certain flow conditions is clarified, and the heat transfer geometrical parameters of the metal foam-filled radiators and their heat transfer performance are obtained.

2. Materials and Methods

2.1. Heat Accounting for Radiators

The heat of the hot and cold fluids is exchanged through the solid walls. First, the hot fluid conducts the heat to the solid walls; next, it is conducted via one side of the solid walls toward the other side, and then the heat is transferred to the cold fluid via the walls. Overall, the heat exchange can be distinguished as a heat giving–heat conducting–heat giving process acting in tandem.

If a hot fluid flows in a metal foam or radiator, a cold fluid passes through the metal foam or radiator, and convection occurs to dissipate the heat. Based on the heat balance principle, it is clear that when the ducts are well insulated, then the amount of heat discharged per unit time of the hot flow and the amount of heat absorbed per unit time of the cold flow are equal.

For a radiator with hot and cold fluids flowing against each other, the heat balance equation reads as follows:

$$Q = q_{m,c}(H_{c,2} - H_{c,1}) = q_{m,h}(H_{h,1} - H_{h,2}). \tag{1}$$

Here, $q_{m,c}$ and q_{mhh} indicate the mass flow rate of the cold and hot fluids, respectively; H_c and H_h correspond to the enthalpy per unit of cold and hot fluid (the subscripts c for cold and h for hot) and the subscripts "1" and "2" correspond to the inlet and outlet side of each unit.

If there is no phase change in either the hot or cold fluid inside the radiator, and the specific heat coefficient at constant pressure.of the fluid, c_p, does not change due to a change in the temperature, then Equation (1) can be expressed as follows:

$$Q = q_{m,c}c_{p,c}\left(t''_1 - t'_1\right) = q_{m,h}c_{p,h}\left(t'_2 - t''_2\right) \tag{2}$$

For overall heat transfer, the heat transfer equation required is as follows:

$$Q = kA\Delta t_m. \tag{3}$$

Here, A is the contact area; Δt_m represents the average temperature difference between the two ends where the fluid is located, i.e.,

$$\Delta t_m = \frac{\Delta t_h - \Delta t_c}{ln(\Delta t_c \Delta t_h)}\left(\Delta t_c = t''_1 - t'_1; \Delta t_h = t'_2 - t''_2\right) \tag{4}$$

While K is the heat transfer coefficient, the introduction of Equation (3) into Equation (1) and the association of Equations (1) and (2) lead to the following:

$$k = \frac{q_{m,c}c_{p,c}(t''_c - t'_c)}{A\Delta t_m} = \frac{q_{m,h}c_{p,h}(t'_h - t''_h)}{A\Delta t_m}. \tag{5}$$

According to this Equation, it is clear that determining the inlet and outlet temperatures of the two fluids and the flow rate of the radiator suffices to obtain the total heat transfer coefficient, K.

During actual operation, the heat dissipation as well as the heat absorption achieved by the hot and cold fluids are not in an absolutely equal state and need to be based on the heat balance theory to obtain their relative error in heat balance ΔQ as follows:

$$\Delta Q = \frac{(Q_h - Q_c)}{Q_c} \times 100\%. \tag{6}$$

Here, Q_h denotes fluid heat release and Q_c denotes fluid heat absorption; in the case of $\Delta Q < 5\%$, it can be assumed that the system is in a state of thermal equilibrium.

Forced convection is applied to the fluid in the radiator. The factors that will have an effect on the heat transfer coefficient correspond to the internal diameter of the radiator channel D, the fluid flow rate v, the fluid viscosity μ, the fluid density ρ, the fluid heat capacity c_p, the fluid thermal conductivity k, etc. The expression is as follows:

$$h = f\left(l, D, \rho, \mu, c_p, k, v\right). \tag{7}$$

Implementing the measure analysis based on Buckingham's π theorem results in the following:

$$h = f\left(l, D, \rho, \mu, c_p, k, v\right), \tag{8}$$

$$\pi_2 = \frac{Dv\rho}{\mu} = Re, \tag{9}$$

$$\pi_3 = \frac{\mu c_p}{k} = Pr. \tag{10}$$

Therefore, Equation (7) can be related as follows:

$$Nu = f_1(Re, Pr). \tag{11}$$

From heat transfer and fluid mechanics, the Nusselt and Prandtl numbers for the flow of a work mass in an electronic heat sink component are known.

Where d_e is the equivalent diameter of the flow channel or the so-called hydraulic diameter, h denotes the convection heat transfer coefficient and λ denotes the thermal conductivity of water. ρ and μ denotes fluid density and viscosity; c_p denotes constant pressure heat capacity.

2.2. Experimental Materials

This paper focuses on the experimental study of copper foam fin radiators with 10 PPI and 20 PPI (as shown in Figure 1). The experimental components used the following dimensions: length 75 mm, width 45 mm and height 17 mm of copper foam radiator, with a base material thickness of 3 mm. The copper foam was cut to the required size using a cutting machine, cleaned with alcohol to remove oil and dust from the surface and then welded to the substrate. The porosity of the copper foam was 96% and the pore density was 10 PPI and 20 PPI, respectively, while the porosity of the aluminum foam was 96% and the pore density was 10 PPI (as shown in Figure 1). The physical properties are shown in Table 1.

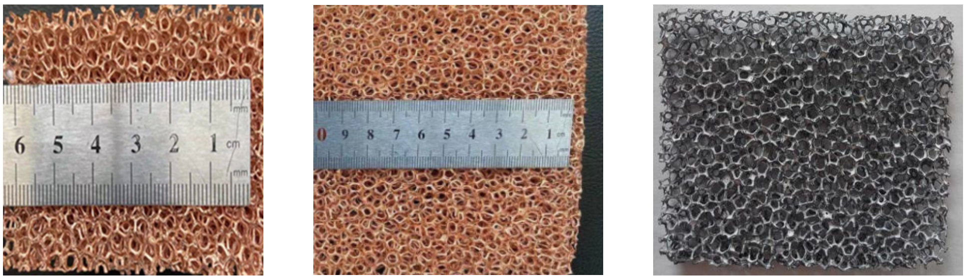

(**a**) (**b**) (**c**)

Figure 1. Copper foam and aluminum foam. (**a**) Copper foam of 10 PPI. (**b**) Copper foam of 20 PPI. (**c**) Aluminum foam of 10 PPI.

Table 1. Physical properties of copper foam and aluminum foam.

Physical Properties / Materials	Pore Density (PPI)	ε	Average Pore Diameter (mm)	Density (g/cm^3)	Thermal Conductivity (W/m·K)	Specific Surface Area (g/m^2)
Copper foam	10	0.96	2.54	0.26	46.21	375
	20	0.96	1.27	0.32	62.56	624
Aluminum foam	10	0.96	2.54	0.09	26.74	375

This paper investigates a copper foam fin radiator at 100 W heating power. The water flow rate was from 10 to 60 L/h and the fins were aligned at 90 degrees to the direction of the water flow. The purpose of this arrangement is to increase the contact surface. The materials filled for the experiments had a pore density of 10 PPI copper metal foam, 10 PPI aluminum metal foam and 20 PPI copper metal foam, as shown in Table 2. The model diagram of the electronic heat sink is shown in Figure 2.

Table 2. Type of material used in the experiment.

Radiator Number	Filling Material Number			
	10 PPI Copper Foam	10 PPI Aluminum Foam	20 PPI Copper Foam	Unfilled
Finless	1	2	3	4
Two fins	1	2	3	4
Triple fins	1	2	3	4
Five fins	1	2	3	4

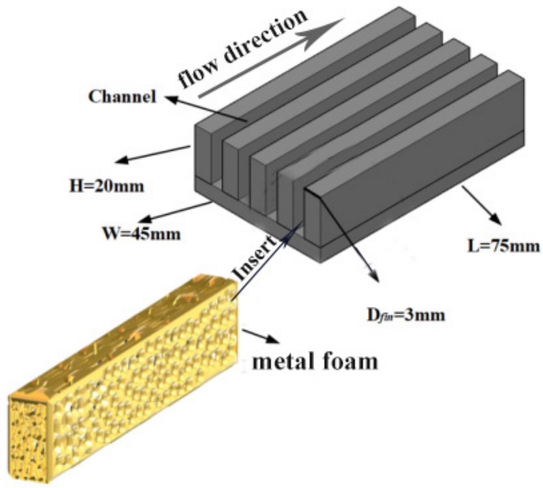

Figure 2. Model diagram of electronic radiator.

2.3. Experimental Setup

The setup contains instruments such as a miniature water pump, an electronic pressure regulator, a paperless recorder, an electrical parameter measuring instrument, a differential pressure transmitter, a constant temperature water bath and a rotameter. A flow chart of the apparatus is shown in Figure 3.

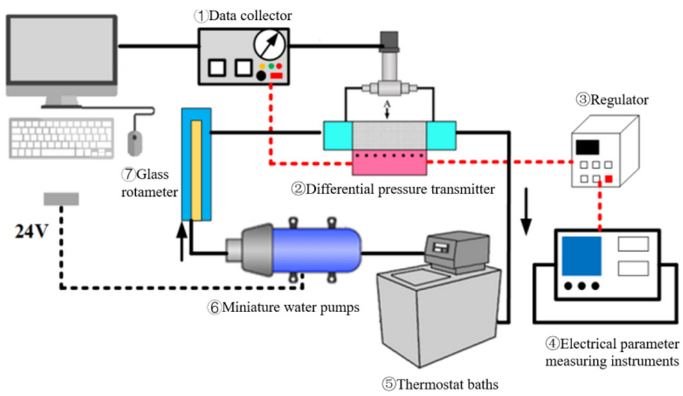

Figure 3. Schematic diagram of experimental process. ① Data collector ② Differential pressure transmitter ③ Regulator ④ Electrical parameter measuring instruments ⑤ Thermostat bath ⑥ Miniature water pumps ⑦ Glass rotameter.

The specific parameters of the main instruments and equipment required in the experiment are as follows: armored thermocouples; miniature water pump, Degree New Weicheng Technology Co., Zhuhai, China; silicon-controlled electronic voltage regulator, Shanghai Steadyford Electric Co., Shanghai, China; paperless recorder, Yokogawa Corporation, Japan; electric parameter measuring instrument, Hangzhou Yuanfang Photoelectric Information Co., Hangzhou, China; differential pressure transmitter, Foshan Yizhong Sensing Instrument Co., Foshan, China; constant temperature water bath, Nanjing Xian'ou

Instrument Manufacturing Co., Nanjing, China; glass rotor flowmeter, Leerda Instruments Co., Portland, OR, USA.

The length of the electronic heat sink was 75 mm and the cross-sectional area was 45 mm × 20 mm. The metal foam of different pore densities were filled into the electronic heat sink. The experimental process is as follows: Water with a constant temperature (20 °C) is fed into the test section through a rotameter. In the test section and the fins (as shown in Figure 4), the heating plate transfers its own heat to the electronic heat sink through thermal conduction and then exchanges heat with the water. Finally, the heat is discharged from the outlet with the flow of water.

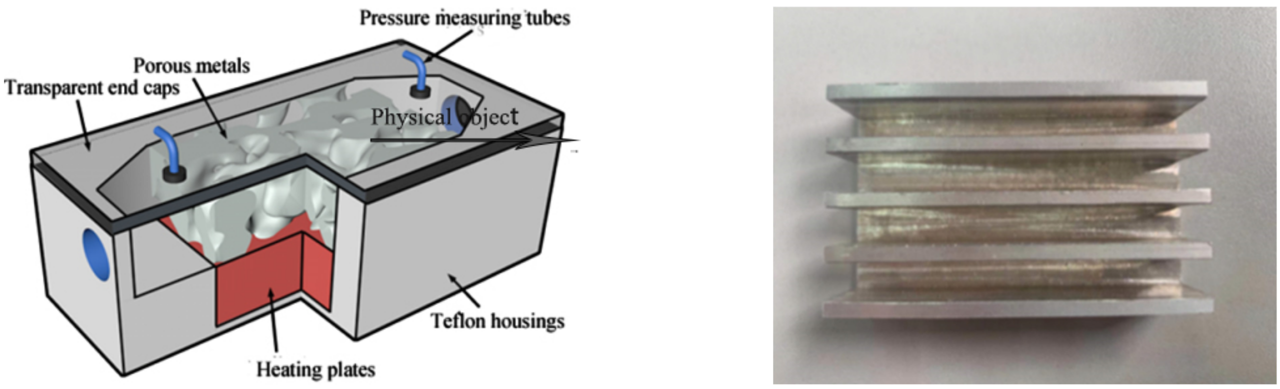

(**a**) (**b**)

Figure 4. Test section renderings and the five fins. (**a**) Test section renderings. (**b**) Physical object of five fins.

3. Results and Discussion

3.1. Data Processing Content

This experiment uses the Wilson graphical method to process the data, and thus, derive the convective heat transfer coefficient. The main data to be measured as well as processed are as follows:

(1) To investigate the total heat transfer performance of a heat sink with a metal foam filling.
(2) To investigate the heat transfer performance and to obtain the Nu–Re relationship curves.
(3) To investigate the resistance performance, obtaining the relationship curves between f-Re, Δp-v.
(4) To evaluate the comprehensive enhanced heat transfer performance of the metal foam-filled electronic heat sinks.

3.2. Data Processing Steps

The experiment requires that we record the raw data and process them as follows.

The average temperature, feature size and feature velocity are calculated, and the corresponding physical parameters are obtained.

(1) The average temperature t_0 for convective heat transfer flowing in the channels of the electronic heat sink parts is as follows:

$$t_0 = (t_1 + t_2 + t_3 + \cdots + t_n)/n. \quad (12)$$

where t_0 is the average temperature of the radiator surface; t_1, t_2 … t_n are the radiator surface temperature, °C.

(2) Feature dimensions refer to standard-like geometric dimensions. Convective heat transfer within the electronic heat sink is dimensioned as a microchannel. This experiment is a rectangular cross section, so the equivalent diameter d_e is as follows:

$$d_e = 4\frac{S}{U} = 2\frac{ab}{a+b}. \quad (13)$$

where d_e is the equivalent diameter of the flow channel or the so-called hydraulic diameter; S is the effective cross-sectional area of the flow channel also known as the cross-flow cross-sectional area, m^2; U is the electronic heat sink parts section perimeter, and fluid contact with the solid wall perimeter, m and a, b are the length and width of the micro-channel cross-section, m.

(3) The characteristic velocity in a heat exchanger can be obtained by taking the flow rate and the cross-flow area. The ratio between the two is the characteristic velocity.

In order to obtain the total convective heat transfer Q during the experiment, the heat transfer coefficient h needs to be determined. The total heat was obtained using Equation (2) and averaged when the heat absorbed by the cold fluid was in equilibrium with that of the hot fluid (ΔQ < 5%). The log-average temperature difference is calculated using Equation (3) and the total heat transfer coefficient K is calculated from Equation (4).

$$Q = qA = h\Delta TA = \rho v c_p(t_{out} - t_{in}). \quad (14)$$

Known from fluid mechanics, the equation for the resistance coefficient of a medium flowing through a system is as follows:

$$f = \frac{\Delta p}{\frac{1}{2}\rho v^2} \cdot \frac{d_e}{l} \quad (15)$$

where Δp is the pressure drop in the experimental section measured by the differential pressure transmitter in the experiment; v is the average flow rate of the tube and l is the distance between the static pressure measurement in the experimental section (110 mm for this experiment).

The resistance coefficients for each group of experiments were fitted using the least squares method as shown in (18) as follows:

$$f = C_f Re^x \quad (16)$$

3.3. Data Processing Results and Performance Curve Analysis

3.3.1. Analytical Comparison of the Total Heat Transfer Coefficient K Versus Flow Rate v

As shown in Figure 5, the heat transfer in the foam-filled electronic heat sink is significantly higher than that of the unfilled heat sink. In the case of a foam-filled electronic heat sink, the heat transfer differs for different pore densities of the metal foam. As the pore density increases, the contact area between the metal foam and the fluid increases, and the total heat transfer area of the heat sink increases. On the other hand, the heat transfer of an electronic heat sink is also related to the metal foam it is filled with. The thermal conductivity of the copper metal foam is higher than that of the aluminum metal foam. Hence, the heat transfer is higher in the same model for the heat sinks filled with copper metal foam material at the same speed conditions.

Equation (16) was used to obtain the relation curve of the heat transfer coefficient K and v of the radiator. As shown in Figure 6, the convective heat transfer coefficient increases by around 31.57% when the number of electronic radiator fins is increased from no fins to two fins. When the number of fins is increased from two to three, the convective heat transfer coefficient increases by about 26.08%. When the number of fins is increased from three to five, the convective heat transfer coefficient decreases, as shown in Figure 7. This is due to an increase in the number of fins accompanied by a decrease in fin spacing and interference in the thermal boundary layer between adjacent fins, resulting in a delay in heat transfer. As a result, there is a maximum number of fins that allows the radiator to achieve optimum heat transfer. As can be seen from the graph, the overall heat transfer coefficient is best when the number of fins is three.

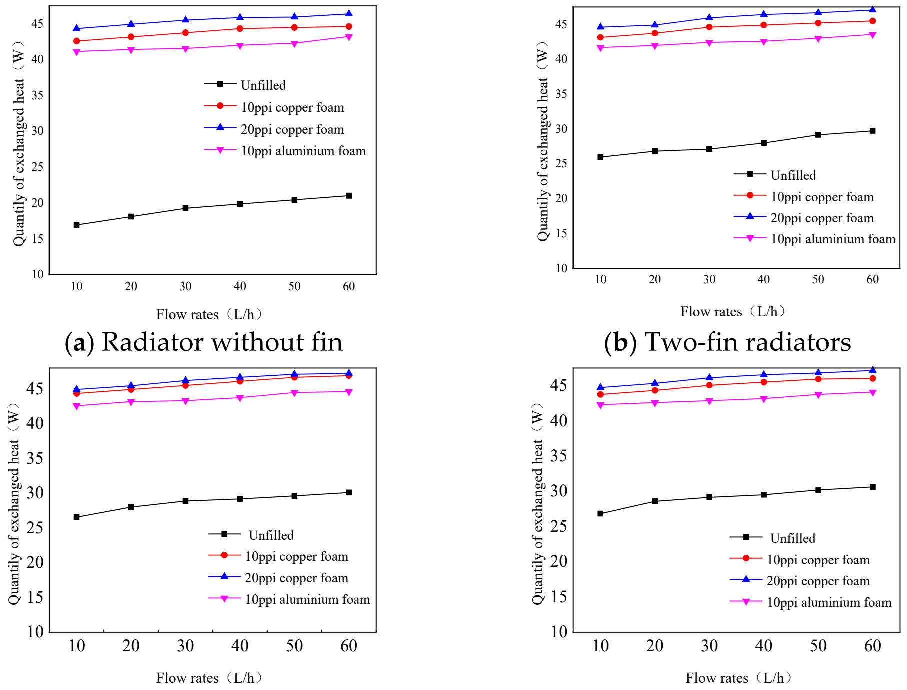

(**a**) Radiator without fin (**b**) Two-fin radiators

(**c**) Three-fin radiators (**d**) Five-fin radiators

Figure 5. The relationship between heat transfer Q and v of radiator.

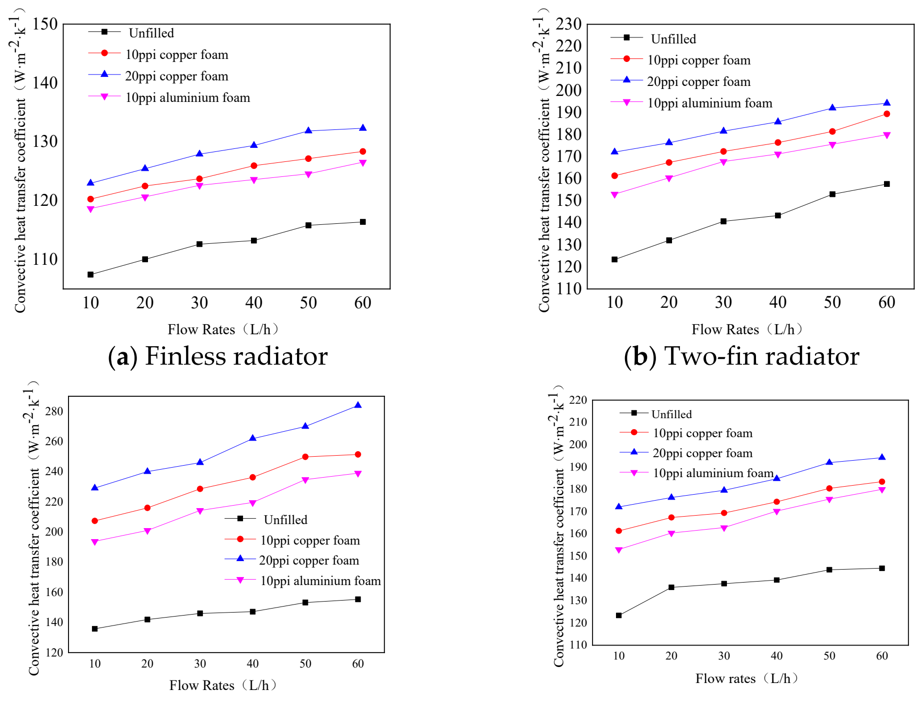

(**a**) Finless radiator (**b**) Two-fin radiator

(**c**) Three-fin radiator (**d**) Five-fin radiator

Figure 6. Relation curve of heat transfer coefficient K and v of radiator.

On the other hand, the convective heat transfer coefficients with and without metal foam filling are very different for the same number of finned electronic heat exchangers. The heat transfer coefficient is significantly higher for the foam-filled type of electronic heat sink than for the unfilled type. Moreover, the convective heat transfer coefficient is also related to the pore density of the filled metal foam, which is related to the length of the pore diameter. The greater the pore density, the smaller the corresponding pore length, and the smaller the diameter of the metal foam skeleton. When the porosity of the metal foam is certain, the contact area between the fluid flowing through the metal foam and the solid also increases, thus strengthening the heat transfer capacity of the electronic heat sink. At the same time, the greater the density of the pores, the greater the disruption of the skeleton within the metal foam and the greater the disturbance caused to the fluid flow, which, in turn, enhances the convective heat transfer intensity. Based on the experimental results, it can be concluded that the highest convective heat transfer coefficient is obtained for copper metal foam with a filled pore density of 20 PPI at a fin number of three.

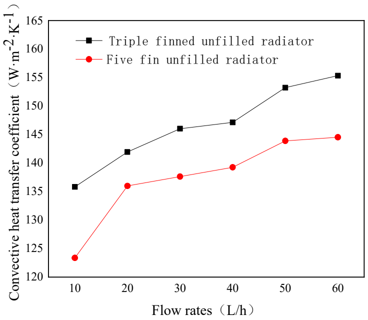

Figure 7. Curve of k versus v for radiators with different numbers of fins.

Equation (2) was used to obtain the heat transfer rate of the radiator. In Figure 8, the heat exchange increasing rate decreases with the increasing flow rate. This is due to the fact that the greater the fluid flow velocity, the greater the degree of turbulence. This results in a consequent decrease in the heat transfer rate. As can be seen from Figure 8, the greatest increase in the heat transfer is in the finless radiator. This is due to the specific surface area of the metal foam itself. The larger the area of contact between the fluid and the solid, the larger the heat transfer area will be, ultimately increasing the heat transfer effect.

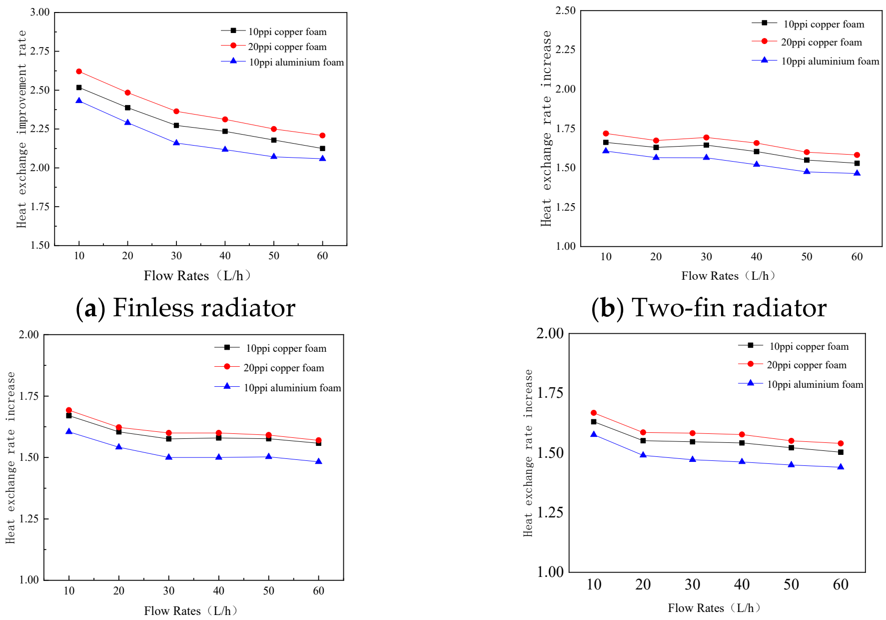

(**a**) Finless radiator (**b**) Two-fin radiator

(**c**) Three fins (**d**) Five fins

Figure 8. Heat transfer rate of radiator.

Electronic heat sink components with different numbers of pieces are filled with materials of the same porosity and different porosity densities. The rate of increase in the convective heat transfer coefficient gradually decreases when the fluid flow rate is in the range from 10 to 30 L/h. The convective heat transfer coefficient improvement rate gradually increases when the fluid flow rate is in the range of 30–60 L/h. When the fluid flow rate is in the range of 30–60 L/h, the convective heat transfer coefficient improvement rate gradually increases. This indicates that after filling the electronic heat sink components with metal foam, the effect of the enhanced heat transfer is more pronounced at low turbulence and less effective at high turbulence. This is because the main effect of the filled metal foam is to create a cyclonic flow in the core part of the flow. At low flow rates, the metal foam promotes a degree of turbulence and thus enhances heat transfer more effectively. At high flow rates, however, turbulence is sufficiently developed, and the enhanced effect of filling with metal foam on the heat transfer in the flow is reduced.

3.3.2. Analytical Comparison of Nusselt Number Nu with Re and Pressure Drop Δp with v

As shown in Figure 9, the pressure drop across the different models of radiators increases with increasing inlet flow, and the trend of increase can be seen as approximately linear. This is due to the fact that at low inlet flow rates, the dominant flow pattern within the radiator is the laminar flow. As the inlet flow rate increases, the flow pattern within the radiator gradually changes to turbulent flow. The filling of the metal foam increases the flow disturbance within the radiator. This ultimately leads to an increase in the resistance to fluid flow, which, in turn, increases the pressure drop between the inlet and the outlet. For the same inlet flow rate, the pressure drop in the electronic radiator increases with the number of fins contained. However, at a certain inlet flow rate, the difference in pressure drop between different types of electronic heat sink is not significant. This is because the pressure drop generated by the fluid flowing through the electronic heat sink depends primarily on the metal foam itself. Moreover, the increase in the number of fins in practice results in the decrease in the fin spacing, thus, in effect, changing the width of the contact cross-section of the fluid in the direction of movement. This ultimately leads to an uneven velocity distribution of the fluid at the inlet. The pressure drop generated by the electronic heat sink also depends on the pore density of the filled metal foam. The greater the pore density, the more chaotic the metal foam's own skeleton structure becomes, which, in turn, generates greater pressure losses.

Equation (11) was used to obtain the relation curve between the Nu and Re of the radiator. As shown in Figure 10, the Nusselt number of the electronic heat sink filled with metal foam is significantly higher than the Nusselt number of the electronic heat sink not filled with metal foam. This indicates that the heat transfer capability of the heat sink filled with metal foam is enhanced. The heat transfer strength of each type of heat sink also differs under different conditions of the Reynolds number. As it can be seen from Figure 10, the Nusselt number increases with the increasing Reynolds number. Additionally, the Nusselt number increases with the increasing pore density at different pore densities, while it increases and then decreases with the number of fins contained in the electronic heat sink. As can also be concluded from Figure 10 that the Nusselt number reaches a maximum when the number of fins is three. This trend is consistent with that shown by the convective heat transfer coefficient.

Equation (16) was used to obtain the radiator resistance coefficient f and Re relation curve. As shown in Figure 11, the frictional drag coefficient gradually decreases as the Reynolds number increases. As $Re > 3000$, the trend of the decreasing frictional drag coefficient becomes progressively slower. The coefficient of frictional resistance and the Reynolds number follow the same trend for electronic heat sinks with and without metal foam filling. The drag coefficient of the electronic heat sink with metal foam filling is significantly higher than that of the electronic heat sink without metal foam filling, due to the structure of the filling metal foam itself.

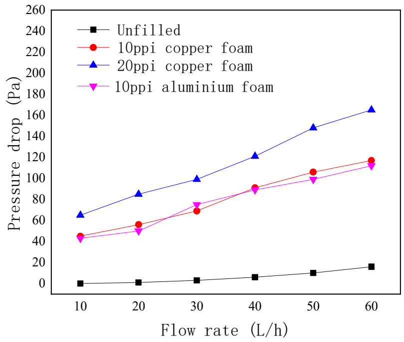

(**a**) Finless

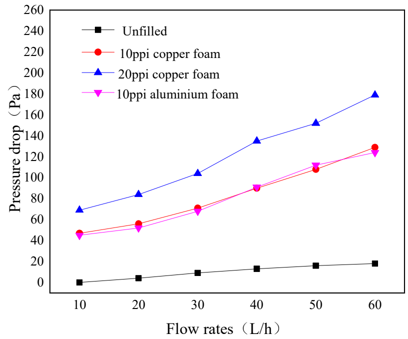

(**b**) Two fins

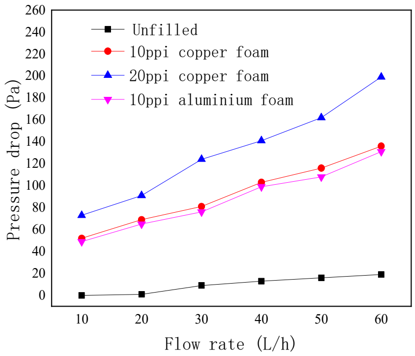

(**c**) Three fins

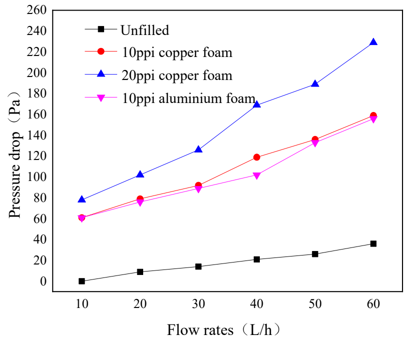

(**d**) Five fins

Figure 9. Radiator pressure drop Δp and v curve.

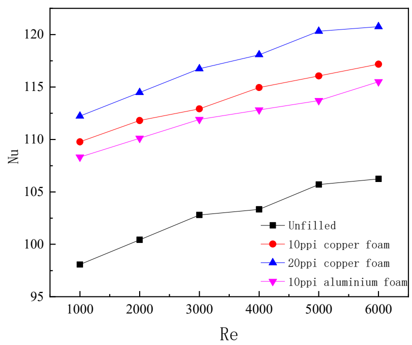

(**a**) Finless

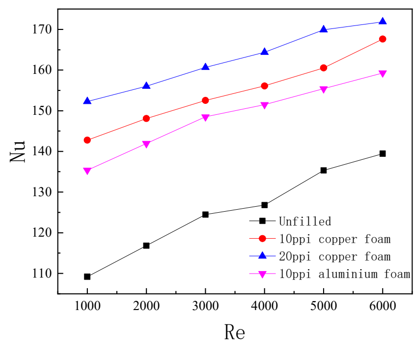

(**b**) Two fins

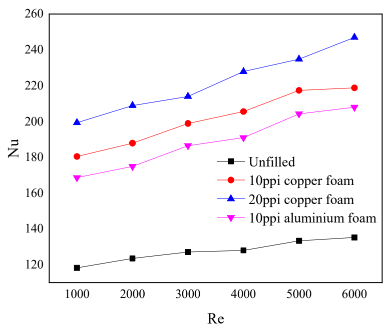

(**c**) Triple fins

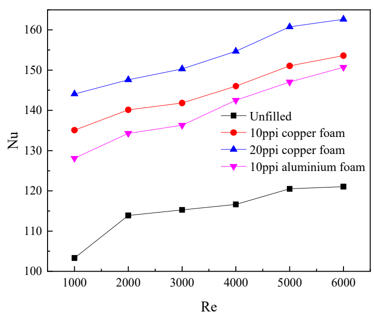

(**d**) Five fins

Figure 10. Relation curve between *Nu* and *Re* of radiator.

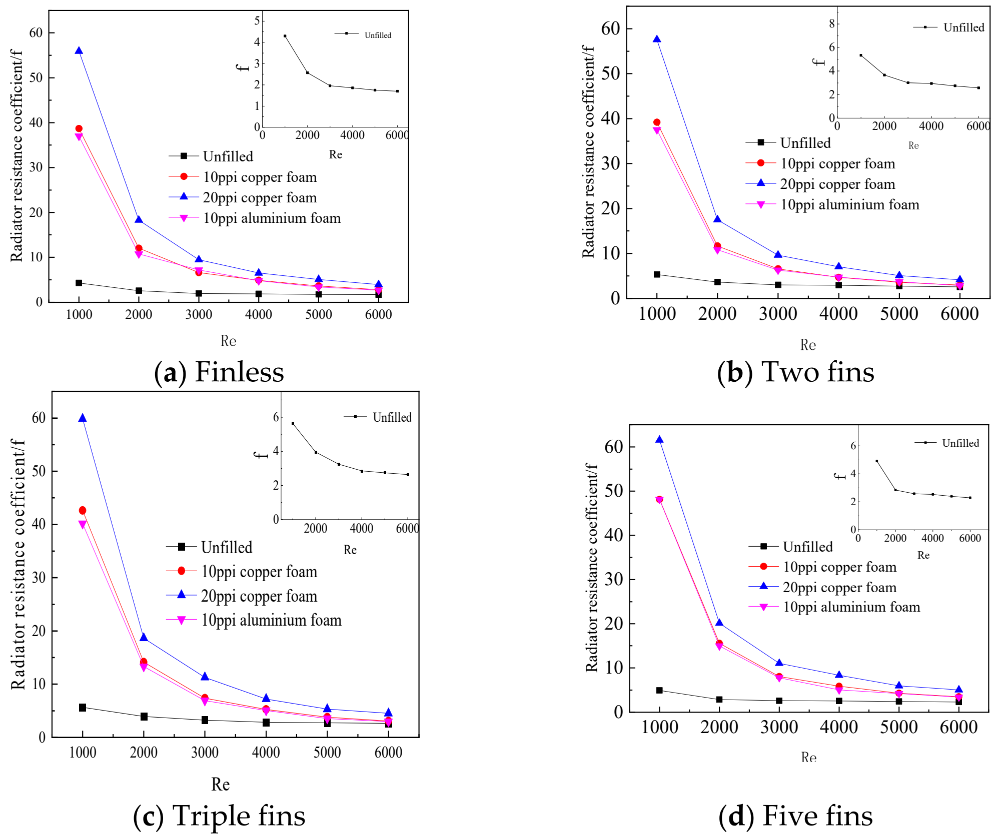

Figure 11. Radiator resistance coefficient of f and Re relation curve.

4. Conclusions

Our experimental studies of electronic heat sinks filled with and without metal foam led to the following conclusions.

Within the specified flow rate range (10 L/h to 60 L/h), the convective heat transfer coefficients of both unfilled and filled electronic heat sinks gradually increase as the fluid flow rate increases. However, the convective heat transfer coefficient of the filled electronic heat sink is significantly higher than that of the unfilled electronic heat sink. As the number of fins in an electronic heat sink increase, the convective heat transfer coefficient tends to increase and then decrease. Additionally, the convective heat transfer coefficient is the highest when the number of fins is three.

For metal foam-filled electronic heat sinks, the rate of increase in the heat transfer coefficient gradually decreases as the flow rate increases. The rate of increase in the convective heat transfer coefficient decreases when the fluid flow rate is in the range from 10 to 30 L/h. The rate of increase in the convective heat transfer coefficient gradually increases when the fluid flow rate is between 30 and 60 L/h.

Within the specified range of the fluid flow, the pressure drop of the filled metal foam radiator gradually increases with the increase in the fluid flow. Under the same fin conditions, the greater the pore density of the filled metal foam, the greater the pressure drop. However, the effect on the pressure drop is similar when the metal foam is filled with different materials under the same fins. As the number of electronic heat sink fins increases, the pressure drop tends to rise for both the filled and unfilled metal foam.

Within the specified flow range, the Nusselt number gradually increases with the increasing Reynolds number, considering the effect of *Re*. The trend is the same for different pore densities and different radiator fins. The Nusselt number reaches its maximum value when the number of electronic heat sink fins is three. Therefore, the heat transfer capacity of the heat sink reaches its maximum when the number of fins of the electronic heat sink is three.

Author Contributions: Conceptualization, B.L. and R.B.; Formal analysis, B.L. and Z.Z.; Investigation, X.S. and R.W.; Writing—original draft, X.S.; Writing—review & editing, B.L., R.B. and P.E.T. All authors have read and agreed to the published version of the manuscript.

Funding: This research received no external funding.

Data Availability Statement: Not applicable.

Conflicts of Interest: The authors declare no conflict of interest.

Nomenclature

ε	Metal foam porosity (vol %)
$q_{m,c}$	Mass flow of cold fluid (kg·s^{-1})
$q_{m,h}$	Mass flow of hot fluid (kg·s^{-1})
H_c	Enthalpy per unit of cold fluid (J·kg^{-1})
H_h	Enthalpy per unit of thermal fluid (J·kg^{-1})
$c_{p,c}$	Constant pressure heat capacity of cold fluid (J/(kg·K))
$c_{p,h}$	Constant pressure heat capacity of hot fluid (J/(kg·K))
t''_c	Temperature of the cold fluid at the outlet (°C)
t'_c	Temperature of the cold fluid at the inlet (°C)
t'_h	Temperature of the hot fluid at the inlet (°C)
t''_h	Temperature of the hot fluid at the outlet (°C)
A	Contact area (cm^3)
ρ	Fluid density (kg/m^3)
μ	Fluid viscosity coefficient (Pa·s)
Δt_m	Logarithmic mean temperature difference (°C)
Q_h	Fluid heat release (W)
Q_c	Fluid heat absorption (W)
S	Effective cross-sectional area of the flow channel (m^2)
U	Cross-sectional circumference of electronic heat sink parts (m)
a.b	Length and width of the micro-channel cross-section (m)
ΔQ	Relative error in thermal equilibrium
Nu	Nusselt number
Re	Reynolds number
Pr	Prandtl number
d_e	Equivalent diameter of the flow channel (m)
λ	Thermal conductivity of water W/(m·K)
f	Coefficient of frictional resistance
l	Experimental section pressure measurement hole spacing (m)
Δp	Experimental section pressure drop (Pa)
v	Fluid flow velocity (m/s)
k	Fluid thermal conductivity (W m^{-2} K^{-1})
R^2	Correlation coefficient

References

1. Garcia-Moreno, F.; Mukherjee, M.; Solórzano, E.; Banhart, J. Metal foams–towards microcellular materials. *Int. J. Mater. Res.* **2010**, *101*, 1134–1139. [CrossRef]
2. Clyne, T.; Markaki, A.; Tan, J.-C. Mechanical and magnetic properties of metal fibre networks, with and without a polymeric matrix. *Compos. Sci. Technol.* **2005**, *65*, 2492–24999. [CrossRef]
3. Qin, J.; Chen, Q.; Yang, C.; Huang, Y. Research process on property and application of metal porous materials. *J. Alloys Compd.* **2016**, *654*, 39–44. [CrossRef]
4. Wu, S.; Liu, X.; Yeung, K.W.K.; Liu, C.; Yang, X. Biomimetic porous scaffolds for bone tissue engineering. *Mater. Sci. Eng. R Rep.* **2014**, *80*, 1–36. [CrossRef]
5. Singh, R.; Lee, P.D.; Dashwood, R.J.; Lindley, T.C. Titanium foams for biomedical applications: A review. *Mater. Technol.* **2010**, *25*, 127–136. [CrossRef]
6. Bansiddhi, A.; Sargeant, T.; Stupp, S.; Dunand, D. Porous NiTi for bone implants: A review. *Acta Biomater.* **2008**, *4*, 773–782. [CrossRef]
7. Ding, C.; Zhang, C.; Ma, L.; Sharma, A. Numerical investigation on melting behaviour of phase change materials/metal foam composites under hypergravity conditions. *Appl. Therm. Eng.* **2022**, *207*, 118153. [CrossRef]

8. Zhao, C. Review on thermal transport in high porosity cellular metal foams with open cells. *Int. J. Heat Mass Transf.* **2012**, *55*, 3618–3632. [CrossRef]
9. Deng, F.; Li, X.; He, L.; Feng, Y. Experimental evaluation of metal foam for sand control. *J. Pet. Sci. Eng.* **2019**, *176*, 1152–1160. [CrossRef]
10. Brothers, A.; Dunand, D. Amorphous metal foams. *Scr. Mater.* **2006**, *54*, 513–520. [CrossRef]
11. Liu, Y.; He, X.; Deng, C. Self-Piercing Riveting of Metal Foam Sandwich Structures. *Mater. Trans.* **2017**, *58*, 1532–1537. [CrossRef]
12. Xu, C.; Mao, Y.; Hu, Z. Tonal and broadband noise control of an axial-flow fan with metal foams: Design and experimental validation. *Appl. Acoust.* **2017**, *127*, 346–353. [CrossRef]
13. Chen, K.; Wang, X.; Chen, P.; Wen, L. Numerical simulation study on heat transfer enhancement of a heat exchanger wrapped with metal foam. *Energy Rep.* **2022**, *8*, 103–110. [CrossRef]
14. Kim, S.Y.; Paek, J.W.; Kang, B.H. Thermal performance of aluminum-foam heat sinks by forced air cooling. *IEEE Trans. Compon. Packag. Technol.* **2003**, *26*, 262–267.
15. Shen, L.; Xu, S.; Bai, Z.; Wang, Y.; Xie, J. Experimental study on thermal and flow characteristics of metal foam heat pipe radiator. *Int. J. Therm. Sci.* **2021**, *159*, 106572. [CrossRef]
16. Kotresha, B.; Gnanasekaran, N. Numerical Simulations of Fluid Flow and Heat Transfer through Aluminum and Copper Metal Foam Heat Exchanger—A Comparative Study. *Heat Transf. Eng.* **2019**, *41*, 637–649. [CrossRef]
17. Chen, T.; Shu, G.; Tian, H.; Zhao, T.; Zhang, H.; Zhang, Z. Performance evaluation of metal-foam baffle exhaust heat exchanger for waste heat recovery. *Appl. Energy* **2020**, *266*, 114875. [CrossRef]
18. Zhao, C.; Lu, W.; Tassou, S. Thermal analysis on metal-foam filled heat exchangers. Part II: Tube heat exchangers. *Int. J. Heat Mass Transf.* **2006**, *49*, 2762–2770. [CrossRef]
19. Kaur, I.; Singh, P. Critical evaluation of additively manufactured metal lattices for viability in advanced heat exchangers. *Int. J. Heat Mass Transf.* **2021**, *168*, 120858. [CrossRef]
20. Saeedan, M.; Ziaei-Rad, M.; Afshari, E. Metal foam as a turbulent flow distributor in the cooling channels of a PEM fuel cell—A numerical study. *Phys. Scr.* **2019**, *94*, 064002. [CrossRef]
21. Shi, J.; Zheng, G.; Chen, Z.; Dang, C. Experimental study of flow condensation heat transfer in tubes partially filled with hydrophobic annular metal foam. *Int. J. Heat Mass Transf.* **2019**, *136*, 1265–1272. [CrossRef]
22. Wang, Y.; Yu, Y.; Jing, Z.; Wang, C.; Zhou, G.; Zhao, W. Thermal performance of lithium-ion batteries applying forced air cooling with an improved aluminium foam heat sink design. *Int. J. Heat Mass Transf.* **2021**, *167*, 120827. [CrossRef]
23. Hossain, M.S.; Shabani, B. Metal foams application to enhance cooling of open cathode polymer electrolyte membrane fuel cells. *J. Power Sources* **2015**, *295*, 275–291. [CrossRef]
24. Saeedan, M.; Afshari, E.; Ziaei-Rad, M. Modeling and optimization of turbulent flow through PEM fuel cell cooling channels filled with metal foam- a comparison of water and air cooling systems. *Energy Convers. Manag.* **2022**, *258*, 115486. [CrossRef]
25. Alhusseny, A.; Al-Aabidy, Q.; Al-Zurfi, N.; Nasser, A.; Aljanabi, M. Cooling of high-performance electronic equipment using graphite foam heat sinks. *Appl. Therm. Eng.* **2021**, *191*, 116844. [CrossRef]
26. Qi, C.; Chen, T.; Tu, J.; Yan, Y. Effects of metal foam on exergy and entropy of nanofluids in a heat sink applied for thermal management of electronic components. *Int. J. Energy Res.* **2020**, *44*, 10628–10651. [CrossRef]
27. Li, Y.; Gong, L.; Xu, M.; Joshi, Y. Hydraulic and thermal performances of metal foam and pin fin hybrid heat sink. *Appl. Therm. Eng.* **2020**, *166*, 114665. [CrossRef]
28. Li, Y.; Gong, L.; Xu, M.; Joshi, Y. Thermal Performance Analysis of Biporous Metal Foam Heat Sink. *J. Heat Transf.* **2017**, *139*, 052005. [CrossRef]
29. Hsieh, W.; Wu, J.; Shih, W.; Chiu, W. Experimental investigation of heat-transfer characteristics of aluminum-foam heat sinks. *Int. J. Heat Mass Transf.* **2004**, *47*, 5149–5157. [CrossRef]
30. Liu, J.; Wu, W.; Chiu, W.; Hsieh, W. Measurement and correlation of friction characteristic of flow through foam matrixes. *Exp. Therm. Fluid Sci.* **2006**, *30*, 329–336. [CrossRef]
31. Dukhan, N.; Chen, K.-C. Heat transfer measurements in metal foam subjected to constant heat flux. *Exp. Therm. Fluid Sci.* **2007**, *32*, 624–631. [CrossRef]
32. Boomsma, K.; Poulikakos, D. On the effective thermal conductivity of a three-dimensionally structured fluid-saturated metal foam. *Int. J. Heat Mass Transf.* **2001**, *44*, 827–836. [CrossRef]
33. Shih, W.H.; Chiu, W.C.; Hsieh, W.H. Height Effect on Heat-Transfer Characteristics of Aluminum-Foam Heat Sinks. *J. Heat Transf.* **2006**, *128*, 530–537. [CrossRef]
34. Singh, P.; Nithyanandam, K.; Mahajan, R.L. An experimental and numerical investigation of forced convection in high porosity aluminum foams subjected to jet array impingement in channel-flow. *Int. J. Heat Mass Transf.* **2019**, *149*, 119107. [CrossRef]
35. Bhattacharya, A.; Mahajan, R.L. Finned Metal Foam Heat Sinks for Electronics Cooling in Forced Convection. *J. Electron. Packag.* **2002**, *124*, 155–163. [CrossRef]